VOLUME 115, NUMBER 8
APRIL 21, 1993

JOURNAL
OF THE
AMERICAN
CHEMICAL
SOCIETY

Energetic and Structural Basis for the Preferential Formation of the Native Disulfide Loop Involving Cys-65 and Cys-72 in Synthetic Peptide Fragments Derived from the Sequence of Ribonuclease A

S. Talluri, C. M. Falcomer, and H. A. Scheraga*

Contribution from the Baker Laboratory of Chemistry, Cornell University, Ithaca, New York 14853-1301

Received October 14, 1992

Abstract: Two fragments of ribonuclease A (RNase A), peptides [61–74] and [65–72], were obtained by solid-phase peptide synthesis. Both peptides contain the residues cysteine-65 and cysteine-72 which form a disulfide bond in native RNase A. The free-energy difference for the formation of the Cys-65–Cys-72 disulfide in the two peptides was obtained from the equilibrium constants measured in aqueous solution at 25 °C and pH 8.0 and 9.0; the free-energy difference was close to zero under these conditions. NOESY and ROESY experiments were carried out in DMSO and in aqueous solution by NMR spectroscopy to determine the conformation of the peptide corresponding to residues 61–74 of RNase A. These experiments show that short-range interactions help to stabilize the Cys-65–Cys-72 disulfide bond with the formation of a type-II β-turn involving residues 66–69; this turn is shifted by one residue from the native type-III turn at residues 65–68, as deduced in earlier studies of disulfide-forming equilibria in fragments of RNase A.

Introduction

The amino acid sequence of a protein contains the information necessary to specify its unique three-dimensional structure in the folded state.[1,2] Many proteins contain cysteine residues which are linked to each other by disulfide bonds. The formation of these disulfide bonds does not occur randomly; the sequence of each protein specifies the unique pairing of the disulfide bonds that will be observed in the native state. In several proteins that have been studied, the reduction of one or more disulfide bonds results in a decrease of the free energy difference between the native and denatured forms of the protein.[3-5] The formation of the disulfide bonds between cysteine residues helps to make the low-entropy folded state of the protein more stable than that of the denatured state by reducing the entropy of the denatured state. In order to investigate the importance of local interactions in the preferential formation of native disulfide bonds in proteins, we focused our attention on ribonuclease A (RNase A), particularly on the loop between residues 61 and 74, stabilized by a disulfide bond between Cys-65 and Cys-72.

This loop plays an important role in the enzymatic specificity of RNase A. If the segment of RNase A corresponding to residues 59–73 replaces the corresponding segment of angiogenin (residues 58–70), the resulting hybrid protein has a dramatically higher RNase A-like activity and a dramatically reduced angiogenicity.[6] If this loop in native RNase A is replaced by the sequence that occurs in the corresponding loop of angiogenin, a hybrid-RNase A is obtained that has a greatly diminished catalytic activity against uridyl-(3′-5′)-adenosine (UpA) and slightly increased

(1) Anfinsen, C. B.; Haber, E.; Sela, M.; White, F. H., Jr. *Proc. Natl. Acad. Sci. U.S.A.* **1961**, *47*, 1309–1314.
(2) Anfinsen, C. B.; Scheraga, H. A. *Adv. Protein Chem.* **1975**, *29*, 205–300.
(3) Denton, M. E.; Scheraga, H. A. *J. Protein Chem.* **1991**, *10*, 213–232.
(4) Schwarz, H.; Hinz, H.-J.; Mehlich, A.; Tschesche, H.; Wenzel, H. R. *Biochemistry* **1987**, *26*, 3544–3551.
(5) Talluri, S.; Rothwarf, D. M.; Zheng, Z.; Scheraga, H. A., unpublished results.
(6) Harper, J. W.; Vallee, B. L. *Biochemistry* **1989**, *28*, 1875–1884.

0002-7863/93/1515-3041$04.00/0

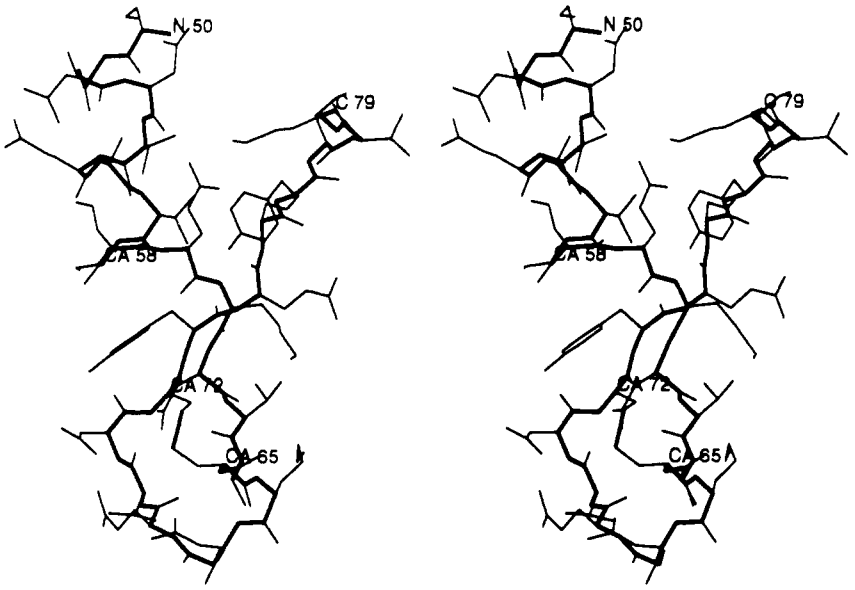

Figure 1. Structure of residues 50–79 of RNase A from Wlodawer et al.[10] The disulfide bond between Cys-65 and Cys-72 is indicated.

efficiency as an inhibitor of translation in vitro, similar to the inhibitory behavior of angiogenin.[7]

The structure of RNase A has been determined by using X-ray crystallography, and a number of highly refined structures of RNase A are available.[8-11] The backbone structure of RNase A has been described in detail by Borkakoti et al.[8] Residues 61–74 form a loop at the end of a β-sheet (Figure 1). Residues 61–64 and residues 71–75 form two strands of a four-strand antiparallel β-sheet. This β-sheet is stabilized by hydrogen bonds between the amide NH of Val-63 and the CO of Cys-72 and between the backbone amide NH of Gln-74 and the CO of Lys-61. Residues Cys-65, Lys-66, Asn-67, and Gly-68 form a type-III β-turn. In this β-turn, the backbone amide NH of Gly-68 forms a hydrogen bond with the CO of Cys-65 and the amide NH of Cys-65 forms a hydrogen bond with the CO of Gln-69. The C^{α} of Gln-69 and the C^{α} of Cys-72 are separated by a distance of 6.98 Å in the structure of RNase A containing uridine–vanadate and obtained by joint refinement of X-ray and neutron diffraction data;[10] this is a type-IV β-turn according to the definition of Lewis et al.[12] However, in the structure of phosphate-free RNase A,[11] the distance between the $C^{\alpha}H$ of Gln-69 and the $C^{\alpha}H$ of Cys-72 is 7.08 Å; this distance is slightly larger than the cutoff of 7 Å used for the definition of a β-turn.[12] The backbone amide NH of Gln-69 forms a hydrogen bond with the side-chain amide carbonyl group of Asn-67. The side-chain amide group of Gln-69 is involved in two side-chain to side-chain hydrogen bonds. The side-chain amide NH of Gln-69 forms a hydrogen bond with the side-chain carbonyl of Asn-71, and the side-chain carbonyl forms a hydrogen bond with the side-chain amide NH of Asn-67. The structure of phosphate-free RNase A has been modeled[11] with two separate side-chain conformations for Lys-61 and Asn-67. One of these two conformers of Lys-61 forms a salt-link to the Glu-9 of another molecule in the crystal lattice. An additional intermolecular hydrogen bond has been found between the carbonyl O of Lys-66 and the N^{δ} of Asn-34.[8]

In our earlier work, based on disulfide exchange equilibrium studies, we established that the formation of the native disulfide bond, 65–72, is thermodynamically preferred over the formation of the non-native disulfide bond, 58–65, in the peptide corresponding to residues 50–79 of RNase A[13] and also in the peptide corresponding to residues 58–72 of RNase A[14] (Figure 2, a and b). The work described here provides a structural basis for the preferential formation of the native disulfide in the peptides [50–79] and [58–72]. Although the native disulfide bond is formed preferentially over the non-native disulfide bond in both of these peptides, the equilibrium constant for the formation of the native and non-native disulfide bonds from the unfolded form is slightly different in the two peptides,[13,14] possibly due to interactions that are present in the longer peptide that are absent in the shorter peptide or due to differences in the pK's of the cysteine thiols. Similar measurements of the disulfide exchange equilibrium on analogs of the peptide [58–72], in which residues Lys-66 and Asn-67 were replaced by Gln and Ala, respectively, led to the proposal that the native turn comprising residues 65–68 is shifted to residues 66–69 in these analogs.[14] We have used NMR spectroscopy to study the solution structure of the terminally-blocked peptide corresponding to residues 61–74 of native RNase

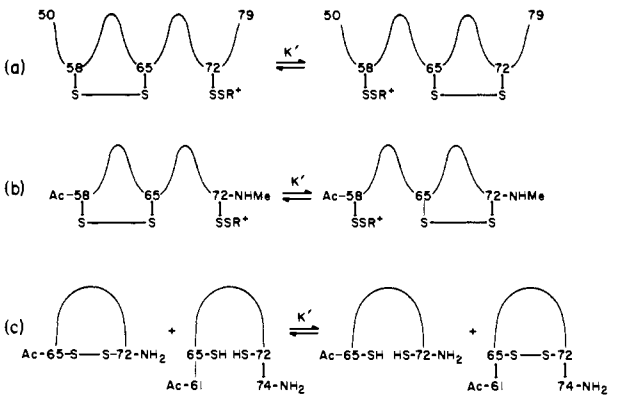

Figure 2. Representation of equilibria in disulfide loops of RNase A fragments: (a) [50–79], with free amino and carboxyl terminal groups;[13] (b) [58–72], with blocked terminal groups;[14] and (c) [65–72] and [61–74], with blocked terminal groups.

(7) Allemann, R. K.; Presnell, S. R.; Benner, S. A. *Protein Eng.* **1991**, *4*, 831–835.
(8) Borkakoti, N.; Moss, D. S.; Palmer, R. A. *Acta Crystallogr.* **1982**, *38B*, 2210–2217.
(9) Wlodawer, A.; Sjölin, L. *Biochemistry* **1983**, *22*, 2720–2728.
(10) Wlodawer, A.; Miller, M.; Sjölin, L. *Proc. Natl. Acad. Sci. U.S.A.* **1983**, *80*, 3628.
(11) Wlodawer, A.; Svensson, L. A.; Sjölin, L.; Gilliland, G. L. *Biochemistry* **1988**, *27*, 2705–2717.
(12) Lewis, P. N.; Momany, F. A.; Scheraga, H. A. *Biochim. Biophys. Acta* **1973**, *303*, 211–229.
(13) Milburn, P. J.; Scheraga, H. A. *J. Protein Chem.* **1988**, *7*, 377–398.
(14) Altmann, K.-H.; Scheraga, H. A. *J. Am. Chem. Soc.* **1990**, *112*, 4926–4931.

A to test this hypothesis. The results of these experiments are discussed below.

Experimental Section

Peptide Synthesis and Purification. Two peptides, Ac-Cys-Lys-Asn-Gly-Gln-Thr-Asn-Cys-NH_2, corresponding to the native fragment 65–72, and Ac-Lys-Asn-Val-Ala-Cys-Lys-Asn-Gly-Gln-Thr-Asn-Cys-Tyr-Gln-NH_2, corresponding to native fragment 61–74, were synthesized manually by a solid-phase procedure. The syntheses started from 100 mg of 4-methylbenzhydrylamine (MBHA) resin with a substitution level in amino groups of 1 mmol/g. The *tert*-butyloxycarbonyl (Boc) group was used for α-amino protection, the acetaminomethyl (Acm) group for thiol protection, the benzyloxycarbonyl (Z) group for protection of the ϵ-amino group of Lys, and benzyl (Bzl) for hydroxyl protection of Thr. Each synthetic step started with deprotection of α-amino groups with 25% trifluoroacetic acid (TFA) in dichloromethane (DCM), followed by washes with DCM, neutralization with 10% triethyl amine (TEA) in DCM, washes with DCM, and coupling with 0.3 mmol of Boc-amino acid and 0.3 mmol of *N,N'*-dicyclohexylcarbodiimide (DCC) in DCM for 90 min. Couplings were monitored by using the Kaiser ninhydrin test[15] and repeated when necessary. Asn and Gln residues were coupled as their hydroxybenzotriazole active esters (0.5 mmol) in dimethylformamide (DMF) to prevent the dehydration of the side-chain amide group. After generation of the desired peptides, the N-terminal amino groups were acetylated, and the resulting peptides were cleaved from the resin by using 2 mL of 10% trifluoromethanesulfonic acid (TFMSA) in TFA in the presence of 0.3 mL of thioanisole/1,2-ethanedithiol (2/1) at 0 °C for 60 min. The linear peptides were recovered by filtration to remove the resin and precipitated with ethyl ether; they were then dissolved in water and lyophylized.

Analytical and preparative scale reverse phase HPLC of the crude peptides were carried out with a Spectra Physics SP 8000 liquid chromatograph coupled to a 770 spectrophotometric detector. Analytical scale RP-HPLC chromatograms were obtained with a Waters RCM 100 radial compression module (Waters Associates) loaded with a Nova-PAK C_{18} 5 mm i.d. cartridge with spectrophotometric detection at 210 nm. Preparative chromatography was carried out with a Rainin Dynamax Macro C_{18} column (Rainin Instrument Co.) with spectrophotometric detection at 220 nm. The flow rates were 1 and 20.0 mL/min for the analytical and preparative scale chromatograms, respectively. Linear gradients of acetonitrile in water, both as 0.09% TFA solutions, were used to achieve the elution of the peptides. The linear gradient, expressed as proportion of acetonitrile (v/v), used for the elution of fragments 65–72 and 61–74 was 5–10% in 30 min.

Cyclization was carried out with I_2/MeOH.[16] The two cyclic fragments were isolated by preparative HPLC using the Rainin Dynamax Macro C_{18} column with spectrophotometric detection at 220 nm. The gradients used were 7–15% in 25 min for cyclic 61–74 and 2–7% in 45 min for cyclic 65–72.

The identity of the two peptides was confirmed by amino acid analysis and by FAB mass spectrometry (Table I).

The bis(thiol)acyclic peptides were prepared from the cyclic disulfides by reduction with DL-dithiothreitol (DTT)[17] and isolated by analytical RP-HPLC; the gradients used were 3–11% in 30 min for acyclic 65–72 and 14–25% in 40 min for acyclic 61–74.

Disulfide-Exchange Equilibrium. Peptides [61–74] and [65–72] differ by the presence of residues 61–64 and 73–74 in the former. In order to determine whether these extra residues play any role in influencing the formation of the native disulfide bond between Cys-65 and Cys-72, we determined the equilibrium constants for the following process at 25 °C, pH 8.0 and 9.0.

$$[61\text{–}74]_r + [65\text{–}72]_{ox} \overset{K'_{8.0\text{–}9.0}}{\rightleftharpoons} [61\text{–}74]_{ox} + [65\text{–}72]_r \qquad (1)$$

The subscripts r and ox denote oxidized and reduced species, respectively, where

$$K'_{8.0\text{–}9.0} = \frac{[61\text{–}74_{ox}][65\text{–}72_r]_o}{[61\text{–}74_r]_o[65\text{–}72_{ox}]} \qquad (2)$$

for the equilibrium observed at both pH 8.0 and 9.0, and $[X_r]$ and $[Y_r]$ are the analytical concentrations of the respective reduced peptides.[17] The zero subscript on $[X_r]$ and $[Y_r]$ indicates the total analytical concentration of all neutral and ionized forms of the reduced species (see eq 3 of ref 17).

The corrections that are required to obtain the value of the pH independent equilibrium constant K' from $K'_{8.0\text{–}9.0}$ are generally small.[17,18] Therefore, we chose to investigate the relative stabilities of the peptides based on the values of the apparent equilibrium constants obtained at pH 8.0 or 9.0, i.e., $K'_{8.0}$ or $K'_{9.0}$.

All of the solutions were prepared, and the disulfide-exchange equilibration experiments were carried out, as described in our previous paper.[17] The disulfide-exchange reaction was quenched by lowering the pH to 2.0 with aqueous TFA (0.3 M). The concentrations of the stock solutions of both the reduced and oxidized peptides were determined by using the photometric NTSB assay.[19] A set of four experiments was carried out using both [61–74] and [65–72] as the actual reductant in two differing mole ratios, i.e., equilibrium was approached from both directions. The quenched equilibrium mixtures were analyzed by elution from a Waters RCM 100 radial compression module loaded with a Nova PAK C18 cartridge. The flow rate was 1 mL/min and the 0.09% TFA acetonitrile/water gradient employed was 3–20% in 60 min. The column effluent was split into two streams; one with a flow of 0.3 mL/min was led to a reaction coil with a total reaction time of 20 min, during which time light was excluded, before reaching the disulfide detection system[20] (DDS) to determine the disulfide content with detection at 412 nm; the other stream was led to the spectrophotometer for detection at 210 nm to determine the peptide concentration.

NMR Spectroscopy. NMR experiments were carried out on either a GE GN500 spectrometer or an XL-400 spectrometer. Two-dimensional NMR experiments were carried out by using a 4 mM solution of the terminally-blocked peptide corresponding to residues 61–74 of RNase A in DMSO, D_2O, and H_2O, respectively. Tetramethylsilane (TMS) was used as a reference in the DMSO solution of the peptide, and 2,2-dimethyl-2-silapentane-5-sulfonate (DSS) was used for the aqueous solutions. The experiments in DMSO were carried out at 20 °C, and the experiments in aqueous solution were carried out at 2.0 °C, unless mentioned otherwise. The pH of the solution was adjusted to 3.5 for the experiments in aqueous solution. DQF-COSY,[21] TOCSY,[22-25] NOESY,[26,27] and ROESY[28,29] spectra were obtained in DMSO and H_2O. The ROESY and TOCSY

Table I. Analytical Data for Peptides [61–74] and [65–72]

peptide	amino acid analysis[a]	FABMS[b] $(M + H)^+$ [c]
61–74 linear	Asn, 3.13; Gln, 2.23; Gly, 1.08; Thr, 1.02; Ala, 1.08; Tyr, 0.56; Val, 1.00; Cys, 1.82; Lys, 2.05	1754.1 (1755.0)
61–74 cyclic	Asn, 3.06; Gln, 2.04; Gly, 1.12; Thr, 1.02; Ala, 1.02; Tyr, 1.01; Val, 0.91; Cys, 1.69; Lys, 2.10	1609.9 (1610.8)
65–72 linear	Asn, 2.10; Gln, 1.11; Gly, 1.14; Thr, 1.05; Cys, 1.53; Lys, 1.05	1050.0 (1051.2)
65–72 cyclic	Asn, 1.97; Gln, 1.15; Gly, 1.07; Thr, 0.99; Cys, 1.88; Lys, 1.05	908.5 (907.0)

[a] Amino acid analyses were carried out at the Biotechnology Analytical and Synthesis Facility at Cornell University. [b] The theoretical mass-to-charge ratio of the protonated molecular ion, including the Ac- and NH_2-terminal groups, is given in parentheses. The Cys residues of the linear peptides were blocked with Acm (acetaminomethyl). FAB mass spectra of peptides 61–74 linear and 61–74 cyclic were obtained in the Mass Spectrometry laboratory, School of Chemical Sciences, University of Illinois. Mass spectral determinations of peptide 65–72 linear and 65–72 cyclic were carried out at the Cornell Mass Spectrometry Facility. [c] Fast-atom bombardment mass spectrometric ratio of mass to charge for the protonated molecular ion $(M + H)^+$.

(15) Kaiser, E.; Colescott, R. L.; Bossinger, C. D.; Cook, P. I. *Anal. Biochem.* **1970**, *34*, 595–598.
(16) Kamber, B. *Helv. Chim. Acta* **1971**, *54*, 927–930.
(17) Milburn, P. J.; Konishi, Y.; Meinwald, Y. C.; Scheraga, H. A. *J. Am. Chem. Soc.* **1987**, *109*, 4486–4496.
(18) Falcomer, C. M.; Meinwald, Y. C.; Choudhary, I.; Talluri, S.; Milburn, P. J.; Clardy, J.; Scheraga, H. A. *J. Am. Chem. Soc.* **1992**, *114*, 4036–4042.
(19) Thannhauser, T. W.; McWherter, C. A.; Scheraga, H. A. *Anal. Biochem.* **1984**, *138*, 181–188.
(20) Thannhauser, T. W.; McWherter, C. A.; Scheraga, H. A. *Anal. Biochem.* **1985**, *149*, 322–330.
(21) Piantini, U.; Sørensen, O. W.; Eich, G. W.; Levitt, M. H.; Bodenhausen, G.; Ernst, R. R. *J. Am. Chem. Soc.* **1982**, *104*, 6800–6801.
(22) Braunschweiler, L.; Ernst, R. R. *J. Magn. Reson.* **1983**, *53*, 521–528.
(23) Shaka, A. J.; Keeler, J.; Frenkiel, T.; Freeman, R. *J. Magn. Reson.* **1983**, *52*, 335–338.
(24) Bax, A.; Davis, D. G. *J. Magn. Reson.* **1985**, *65*, 355–360.
(25) Shaka, A. J.; Lee, C. J.; Pines, A. J. *Magn. Reson.* **1988**, *77*, 274–293.

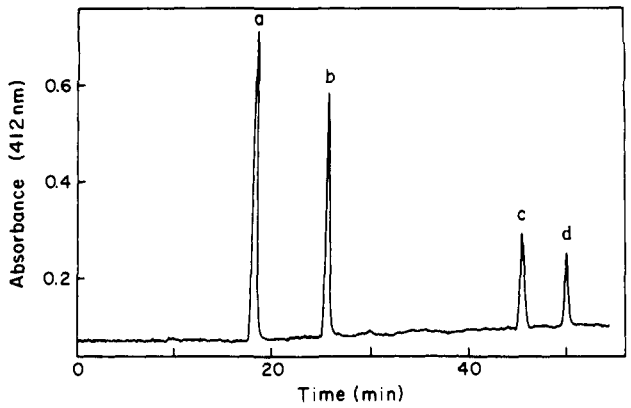

Figure 3. HPLC chromatogram from a disulfide/thiol analysis of the quenched equilibrium mixture between $[65–72]_{ox}$ and $[61–74]_r$. The peptide identities are (a) oxidized [65–72], (b) reduced [65–72], (c) oxidized [61–74], and (d) reduced [61–74].

spectra were obtained on the GN500 spectrometer; for these experiments the spectrometer was reconfigured so that the RF output from the transmitter board was channeled into the decoupler amplifier and then applied to the probe. The composite pulse sequence, DIPSI-2,[30] was used to obtain the TOCSY spectra. The ROESY and TOCSY spectra in H_2O were obtained by using the jump-return-echo method of selective excitation.[31] The DQF-COSY and NOESY spectra in H_2O were obtained by irradiation at the solvent resonance to suppress the H_2O peak. A mixing time of 180 ms was used for the ROESY experiment in DMSO (30 °C) and a mixing time of 250 ms was used for the experiment in H_2O. The temperature dependence of the chemical shifts was obtained from one-dimensional spectra for the amide resonances that were resolved and from two-dimensional spectra for the amide NH resonances that were not resolved in one-dimensional spectra.

Results

Cyclization Equilibrium. A typical chromatogram of an equilibrium mixture for the reaction in Figure 2c is shown in Figure 3. The reduced forms of [61–74] and [65–72] eluted after the respective oxidized forms.

The numerical output from digital integration of the chromatogram was substituted directly into eq 2, yielding the apparent equilibrium constants $K'_{8.0}$ and $K'_{9.0}$. The mean value of $K'_{8.0}$ = 1.08(0.051) was used to calculate the standard Gibbs free energy change, $(\Delta G°)' = -0.046$ kcal mol^{-1}; likewise, $K'_{9.0} = 0.97(0.045)$ gave $(\Delta G°)' = -0.018$ kcal mol^{-1}. The errors expressed in the values of K' are at the 95% confidence level.

Conformational Study of the Peptide Corresponding to Residues 61–74 in DMSO. The ^{1}H-NMR resonances of this peptide were assigned by using the strategy described by Wüthrich.[32] If a peptide can adopt more than one conformation, and if the conformers interconvert slowly on the NMR time scale (i.e., if the barrier to interconversion is greater than 5–10 kcal/mol, we expect to see more than one resonance corresponding to each proton. We were able to assign a single resonance to each proton in the peptide (Table II); therefore, this peptide adopts a single major conformation in solution (i.e., it is conformationally homogenous) or adopts different conformations that interconvert on a time scale rapid enough to result in averaging of the chemical shifts. Large differences in the chemical shifts among residues of the same type (Table II), large variations in the temperature dependence of chemical shifts (Table III), and large chemical shift differences between geminal diastereotopic glycine protons (Table II) show that the peptide is not a statistical coil.[33] ROESY and NOESY spectra were used for the conformational analysis. The NOESY spectrum had a higher signal-to-noise ratio than the ROESY spectrum. However, the ROESY spectrum had several peaks corresponding to side-chain-to-backbone NOE's, that were of very low intensity in the NOESY spectrum. This indicates that the side chains are more flexible than the backbone, i.e., the side-chain atoms have a smaller correlation time than the backbone atoms. A lower value of correlation time is expected to result in a decrease in the intensity of peaks in a NOESY spectrum (as observed); the intensities of NOE peaks in a ROESY experiment are known to be less sensitive to the value of the correlation time.[28] The patterns of NOE intensities involving backbone amide NH and $C^\alpha H$ atoms were very similar in the ROESY and NOESY spectra.

In native RNase A, residues 61–65 and residues 72–74 form two strands of an antiparallel β-sheet. We did not observe any NOE's connecting the stretch of residues from 61–65 to the stretch of residues from 72–74 (Figure 4). Therefore, we conclude that

Table II. ^{1}H Chemical Shifts for the Peptide [61–74] in DMSO at 20 °C[a]

residue	NH	$C^\alpha H$	$C^\beta H$	$C^\gamma H$	others
K61	8.11	4.22	1.51, 1.33	1.67	
N62	8.31	4.55	2.55, 2.44		
V63	7.61	4.15	1.99	0.82, 0.79	
A64	8.09	4.29	1.21		
C65	7.98	4.53	3.15, 2.86		
K66	8.27	4.26	1.51, 1.33	1.67	
N67	8.33	4.31	2.47		
G68	8.57	3.88, 3.40			
Q69	7.68	4.27	1.98, 1.94	2.18	
T70	7.90	4.07	4.07	1.09	
N71	8.01	4.58	2.61		
C72	7.83	4.40	3.04, 2.84		
Y73	8.02	4.36	2.91, 2.83		$C^\delta H$ 7.00;
Q74	7.90	4.12	1.89, 1.74	2.08	$C^\epsilon H$ 6.63

[a] Chemical shifts are in ppm referenced to TMS.

Table III. Temperature Dependence of Chemical Shift of Backbone NH Groups in DMSO and in H_2O

amino acid	$-\delta$(ppb)/K in DMSO	$-\delta$(ppb)/K in H_2O	amino acid	$-\delta$(ppb)/K in DMSO	$-\delta$(ppb)/K in H_2O
K61	6.2	7.9	G68	10.1	7.6
N62	7.2	6.3	Q69	2.3	2.1
V63	3.5	7.9	T70	6.7	8.6
A64	6.0	7.9	N71	3.2	6.4
C65	6.1	8.7	C72	0.2	3.9
K66	6.5	7.5	Y73	5.7	9.8
N67	8.9	8.3	Q74	7.4	7.9

Table IV. ^{1}H Chemical Shifts for the Peptide [61–74] in H_2O at 2.0 °C[a]

residue	NH	$C^\alpha H$	$C^\beta H$	$C^\gamma H$	others
K61	8.45	4.12	1.75, 1.70	1.40	
N62	8.67	4.72	2.71, 2.80		
V63	8.22	4.12	2.09	0.89	
A64	8.51	4.33	1.38		
C65	8.52	4.67	3.18, 2.91		
K66	8.71	4.34	1.86, 1.73	1.47	
N67	8.70	4.52	2.85		
G68	8.72	4.15, 3.72			
Q69	8.00	4.40	2.21, 2.08	2.41	
T70	8.54	4.32	4.25	1.20	
N71	8.60	4.67	2.85		
C72	8.20	4.66	3.08, 2.98		
Y73	8.56	4.60	3.00		$C^\delta H$ 7.14;
Q74	8.45	4.12	2.02, 1.87	2.28	$C^\epsilon H$ 6.84

[a] Chemical shifts are in ppm referenced to DSS.

(26) Jeener, J.; Meier, B. H.; Bachmann, P.; Ernst, R. R. *J. Chem. Phys.* **1979**, *71*, 4546–4553.
(27) Macura, S.; Ernst, R. R. *Mol. Phys.* **1980**, *41*, 95–117.
(28) Bothner-By, A. A.; Stephens, R. L.; Lee, J.; Warren, C. D.; Jeanloz, R. W. *J. Am. Chem. Soc.* **1984**, *106*, 811–813.
(29) Bax, A.; Davis, D. G. *J. Magn. Reson.* **1985**, *63*, 207–213.
(30) Rucker, S. P.; Shaka, A. J. *Mol. Phys.* **1989**, *68*, 509–517.
(31) Sklenar, V.; Bax, A. *J. Magn. Reson.* **1987**, *74*, 468–471.
(32) Wüthrich, K. *NMR of Proteins and Nucleic Acids*; Wiley-Interscience: New York, 1986; pp 40–161.
(33) Kessler, H. *Angew. Chem., Int. Ed. Engl.* **1982**, *21*, 512–523.

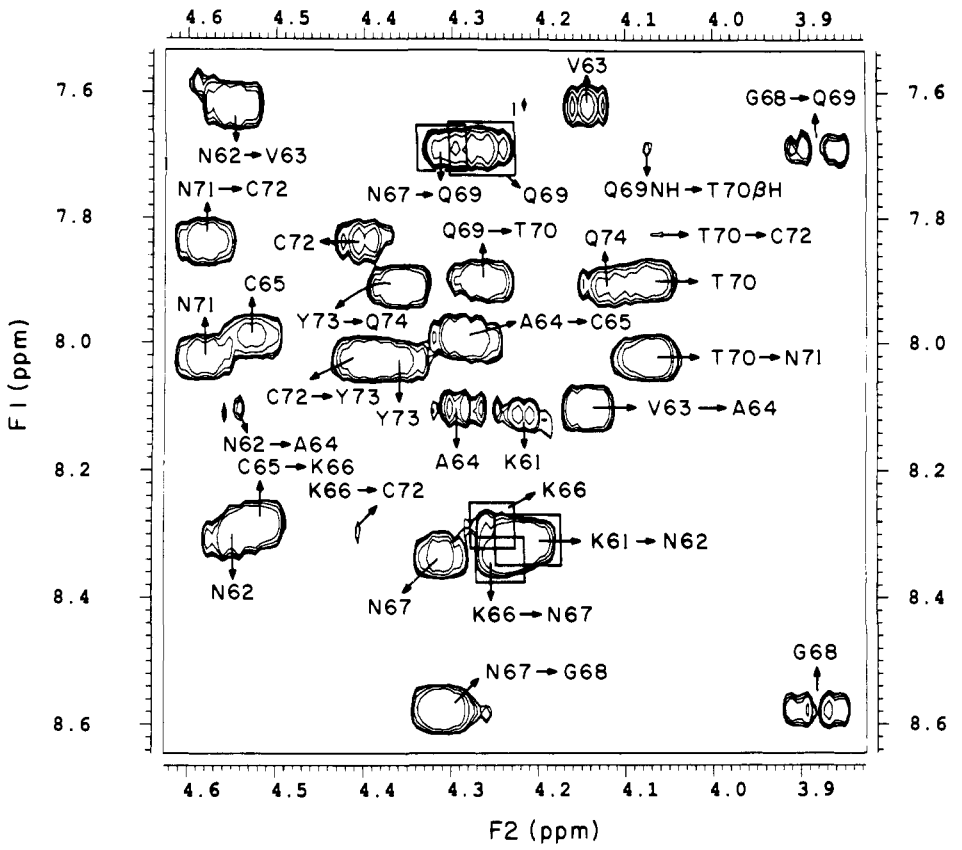

Figure 4. The C$^{\alpha}$H–NH region of the NOESY spectrum of peptide [61–74] in DMSO.

this β-sheet is not formed in this peptide, in DMSO. For an extended chain, we would expect to observe weak sequential NH-(i)–NH(i+1) NOE's. Instead, we observed relatively strong NOE's between the backbone Asn-62 NH and Val-63 NH and also between Val-63 NH and Ala-64 NH, indicating that (unlike in RNase A) the residues between Asn-62 and Ala-64 are not fully extended (Figure 5). In native RNase A, residues 65–68 form a type-III β-turn. If this conformation is significantly populated in this peptide, we would expect to observe an NOE between the C$^{\alpha}$H of Lys-66 and the NH of Gly-68. Gly-68 NH is well-resolved in the spectrum in DMSO, and we did not observe this NOE. In addition, if the native β-turn comprising residues 65–68 exists in this peptide, we would expect the temperature dependence of the chemical shift of Gly-68 NH to be less than –4 ppb/K. The temperature dependence of the chemical shift of Gly-68 is –10.1 ppb/K, the highest (magnitude) among residues 61–74. This indicates that the amide NH of Gly-68 is exposed to the solvent in this peptide. In contrast, Gln-69 has a temperature dependence of the chemical shift of –2.3 ppb/K, indicating a reduced accessibility to the solvent. The data are consistent with the hypothesis that the β-turn has shifted and now consists of the residues 66–69. This hypothesis is further confirmed by the presence of a weak sequential NOE between the backbone amide NH's of Asn-67 and Gly-68 and a strong NOE between the backbone amide NH's of Gly-68 and Gln-69. In addition, we observed a weak NOE peak between Asn-67 C$^{\alpha}$H and the backbone amide NH of Gln-69.

The conformation of residues 70–72 appears to be very similar to that in the native protein. In the native protein, these residues are part of a turn involving residues 69–72. In the X-ray structure of RNase A, the C$^{\alpha}$H of Thr-70 and the amide NH of Cys-72 are separated by a short distance of 3.2 Å. The existence of a similar conformation in solution was confirmed by the presence of a weak NOE between the C$^{\alpha}$H of Thr-70 and the amide NH of Cys-72, by a low-temperature dependence of the chemical shift for the amide NH of Cys-72 (–0.2 ppb/K), and by the presence of strong sequential backbone amide NH–NH peaks involving residues Thr-70, Asn-71, and Cys-72. The i,i+2 peak involving residues Thr-70 and Cys-72 was much weaker in the NOESY spectrum than in the ROESY spectrum, indicating the presence of some conformational mobility in this part of the loop.

These data do not rule out the possible presence of other conformations in solution. In fact, these data do not even prove that the conformation that contains the two native turns is the predominant conformation in solution. However, it is clear that a *significant* number of conformers in the ensemble of conformations in solution contain the two turns described above (66–69 and 69–72); if the ensemble did not contain a significant number of conformers with these two turns, then the non-sequential NOE's between residues Asn-67 and Gln-69 and between residues Thr-70 and Cys-72 would not be observed. Regular backbone structural elements such as α-helix[34-37] or β-turns[38,39] can be detected by the presence of characteristic NOE's (NOE's that are absent in a statistical-coil conformation) or from the solvent or temperature dependence of chemical shifts[34] even if the ensemble of conformations in solution contains only a small fraction of these structures.

Conformational Study of the Peptide Corresponding to Residues 61–74 in Aqueous Solution. The conformation of this peptide in aqueous solution is very similar to that in DMSO. As in the case of DMSO, we found no evidence for the presence of the native type-III β-turn comprising residues 65–68; the data in aqueous solution are consistent with the existence of a β-turn comprising residues 66–69. The amide NH of Gly-68 has a very high

(34) Kim, P. S.; Baldwin, R. L. *Nature* **1984**, *307*, 329–334.
(35) Dyson, H. J.; Rance, M.; Houghten, R. A.; Lerner, R. A.; Wright, P. E. *J. Mol. Biol.* **1988**, *201*, 201–207.
(36) Osterhout, J. J.; Baldwin, R. L.; York, E. J.; Stewart, J. M.; Dyson, H. J.; Wright, P. E. *Biochemistry* **1989**, *28*, 7059–7064.
(37) Jimenez, M. A.; Nieto, J. L.; Herranz, J.; Rico, M.; Santoro, J. *FEBS Lett.* **1987**, *221*, 320–324.
(38) Montelione, G. T.; Arnold, E.; Meinwald, Y. C.; Stimson, E. R.; Denton, J. B.; Huang, S.-G.; Clardy, J.; Scheraga, H. A. *J. Am. Chem. Soc.* **1984**, *106*, 7946–7958.
(39) Dyson, H. J.; Rance, M.; Houghten, R. A.; Lerner, R. A.; Wright, P. E. *J. Mol. Biol.* **1988**, *201*, 161–200.

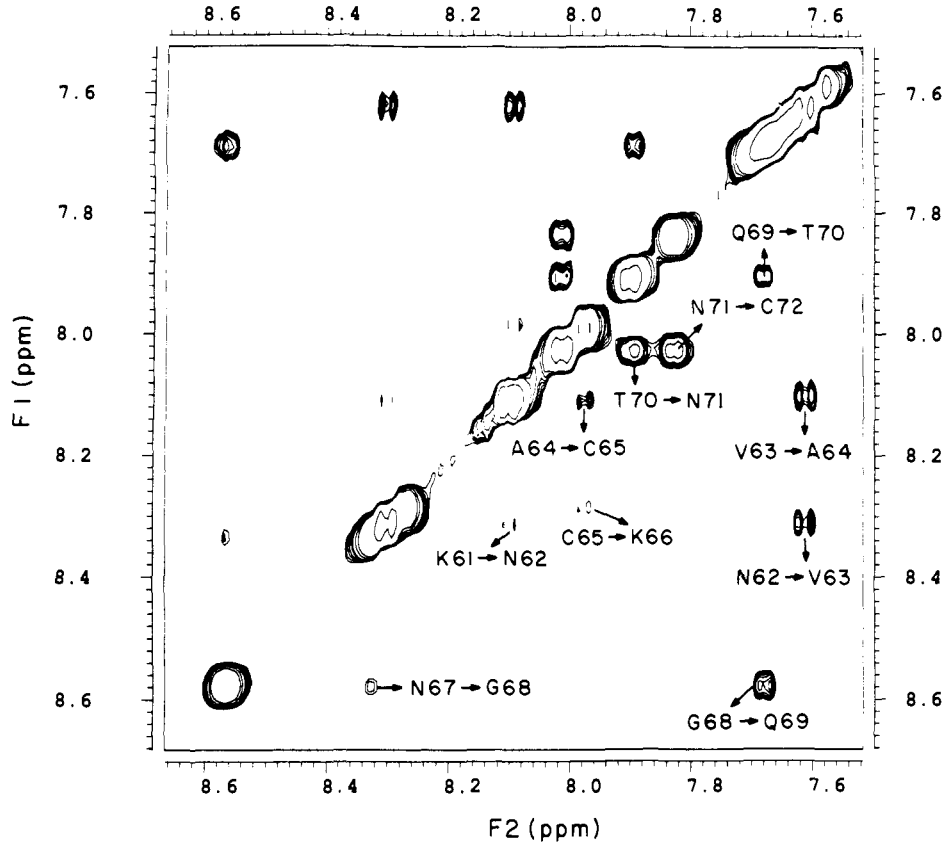

Figure 5. NOESY spectrum of peptide [61–74] in DMSO showing sequential amide NH–NH peaks.

(magnitude) temperature dependence of the chemical shift, –7.6 ppb/K, indicating the absence of any shielding from solvent. On the other hand, the temperature dependence of the chemical shift of the backbone amide NH of Gln-69 was found to be –2.1 ppb/K. The low value of the temperature dependence of the chemical shift indicates that the backbone amide NH of Gln-69 is shielded from solvent, possibly due to hydrogen bonding to the backbone carbonyl oxygen of Asn-67, and that the peptide adopts a β-turn conformation at residues 66–69. This is confirmed by the presence of strong sequential NOE's between the backbone amide NH's of Gly-68 and Gln-69 and a weak non-sequential $i,i+2$ NOE between the $C^{\alpha}H$ of Asn-67 and the backbone amide NH of Gln-69 (Figure 6). A strong sequential $C^{\alpha}H$–NH NOE between residues 67 and 68 (which partially overlaps with the backbone amide NH–$C^{\alpha}H$ NOE peak of Asn-67) suggests that the turn involving residues 66–69 is a type-II β-turn. For a type-II β-turn involving residues 66–69, we would also expect a weak sequential NOE between the backbone amide protons of Asn-67 and Gly-68. We were unable to confirm this because the backbone amide NH chemical shifts of Gly-68 and Asn-67 are very similar. Therefore, our assignment for the type of turn involving residues 66–69 is not completely unambiguous, if data from the H_2O spectrum alone are considered. But, the backbone amide NH chemical shifts of Asn-67 and Gly-68 are better resolved in the DMSO spectrum; therefore, the β-turn involving residues 66–69 can be identified unambiguously as type-II in DMSO, and therefore it presumably exists in water.

Besides the turn involving residues 66–69, we also observed another one, the native turn corresponding to residues 69–72. Evidence for the existence of a turn involving residues 69–72 includes the following: the presence of an NOE between $C^{\alpha}H$ of Thr-70 and the amide NH of Cys-72, strong sequential $i,i+1$ backbone amide NH–NH NOE's between residues Thr-70, Asn-71, and Cys-72, as well as a low-temperature dependence of the chemical shift (–3.9 ppb/K) for the backbone amide NH of Cys-72. In addition to this, we have evidence that the native hydrogen bond between the side-chain NH of Gln-69 and the side-chain carbonyl of Asn-71 is present in H_2O, based on the observation of an NOE between the backbone amide NH of Asn-71 and the $C^{\beta}H$ of Gln-69. In the X-ray structure, the backbone amide NH of Asn-71 and the low $C^{\beta}H$ of Gln-69 are at distances of 2.5 and 3.4 Å, respectively.

To check for the presence of spin-diffusion, we obtained NOESY spectra in D_2O with mixing times of 300, 400, and 500 ms. We did not observe any non-sequential NOE peaks at the longer mixing times that can be ascribed to spin-diffusion. We conclude that spin-diffusion is negligible under these conditions because of the relatively short correlation times expected for a peptide of this size. However, the relative intensities of some $C^{\alpha}H$–$C^{\beta}H^1$ and $C^{\alpha}H$–$C^{\beta}H^2$ peaks changed with the change in mixing time, indicating that there was some spin-diffusion involving these peaks at the longer mixing times; but, these NOE's were not used for conformational analysis.

Discussion

The experiments described in our earlier papers[13,14] show that there is a clear preference for the native disulfide bond involving residues Cys-65 and Cys-72 over the non-native pair Cys-58 and Cys-65. The NMR data for peptide [61–74] presented here show that the preferential formation of the native disulfide bond can be accounted for by the presence of turns involving residues 66–69 and 69–72. The turn involving residues 65–68 that was observed in the crystal structure of the native protein has been shifted to residues 66–69 in the model peptide studied here, [61–74]. We had proposed that this shift occurs in the analogs of the peptide [58–72] in our earlier studies.[14] Empirical conformational energy calculations showed that such a loop would be significantly more stable than the native loop.[14] If Lys-66 is changed to Gln-66 in the peptide [58–72], the tendency of this analog to form the native 65–72 disulfide bond preferentially is not affected.[14] If Gln-66 were at position $i+1$ of a β-turn, this analogue would be expected to show a marked change in its proclivity to form the native disulfide bond. Therefore, these conclusions are also

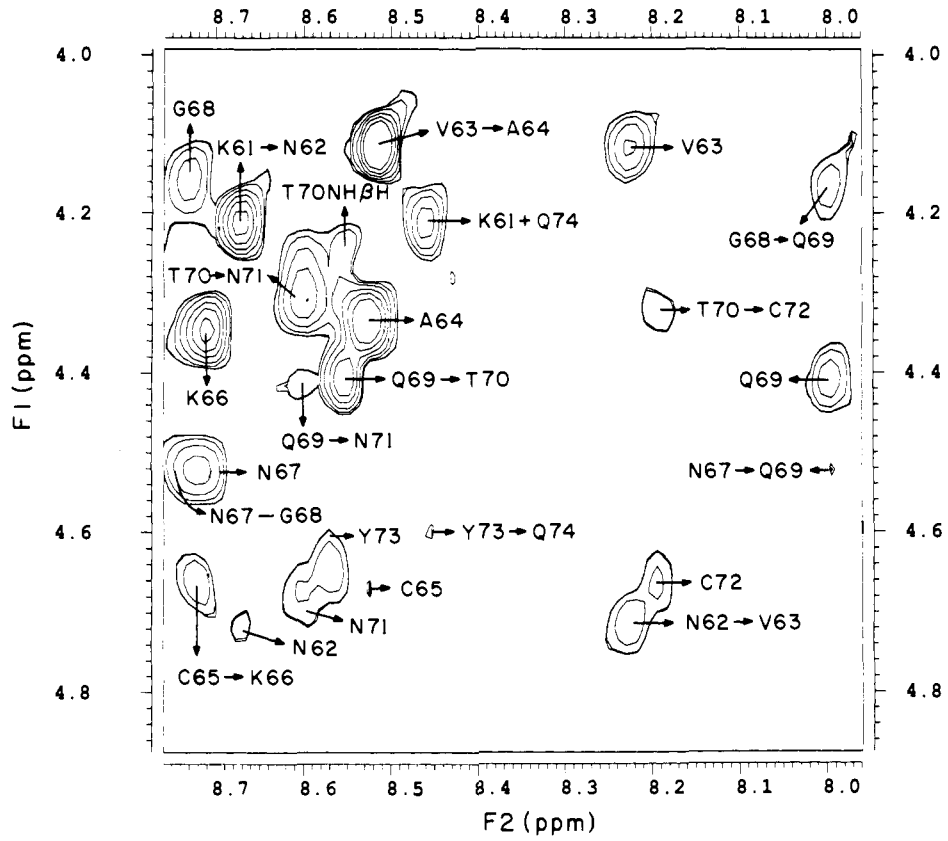

Figure 6. The NH–C$^{\alpha}$H region of the NOESY spectrum of peptide [61–74] in H_2O.

consistent with our earlier proposal,[14] and with the NMR data presented here, that the native turn has shifted by one residue and involves residues 66–69 in these peptides. In addition, we had also previously studied the analog of peptide [58–72] in which Asn-67 was changed to Ala-67 and found that the substitution results in an *increase* in the tendency to form the native disulfide bond.[14] Ala is more likely to be found than Asn in the second position of a β-turn in proteins; therefore, it is possible that a β-turn with Ala at the second position is more stable than a similar β-turn with Asn in the second position; this is the most likely reason for the increase in K' that occurs when Asn-67 is substituted by Ala-67 in peptide [58–72],[14] i.e., a shift in the position of the β-turn.

The equilibrium constant for the preferential formation of the native loop over the non-native loop in the peptide [50–79] is 5.9[13] and the corresponding equilibrium constant for the loop in the peptide [58–72] is 3.6 (Figure 2). The pK's of the thiols of the terminally-blocked terminal cysteine residues (as in the peptide [58–72]) and the cysteine residues that are in the middle of a peptide chain (as in the peptide [50–79]) could be different; this difference could explain the difference in equilibrium constant in the [50–79] and [58–72] peptides. However, the equilibrium constant for the preferential formation of the disulfide bond between the peptides [61–74] (with non-terminal Cys) and 65–72 (with terminal Cys) is close to 1.0 at pH 8.0 and also at pH 9.0 (see Results). Therefore, it is unlikely that the differences in the equilibrium constants for the peptides [58–72] and [50–79] are due to differences in the pK's of cysteine thiols. The additional stabilization of the longer peptide [50–79] over the shorter peptide [58–72] is probably due to interactions with residues that are absent in the shorter peptide, i.e., residues 50–57 and residues 73–79.

Conclusion

NMR spectroscopy and measurements of the equilibrium constants at pH 8.0 and 9.0 have helped us to identify the structural basis for the preferential formation of the native disulfide bond involving residues Cys-65 and Cys-72 in fragments of RNase A and also to explain the differences that we had found earlier in the relative propensity for the formation of the native disulfide bond in these fragments. Thus, while one would expect the entropy of ring closure to be similar in the same size rings (Cys-58 to Cys-65 and Cys-65 to Cys-72), local interactions favor the native loop (Cys-65 to Cys-72); however, the absence of longer-range interactions in these short fragments leads to a shift in the type and position of the β-turn that is dictated by short-range interactions.

Acknowledgment. We thank D. Buckler for helpful discussions. This work was supported by a research grant from the National Institute of General Medical Sciences (GM-24893) of the National Institutes of Health. Support was also received from the National Foundation for Cancer Research.